

## Localized Patterns in Reaction-Diffusion Systems

Shinji KOGA and Yoshiki KURAMOTO

*Department of Physics, Kyoto University, Kyoto 606*

(Received July 26, 1979)

A new chemical pattern is discussed, which is a propagationless solitary island in an infinite medium. We demonstrate analytically its existence and stability for a certain simple model. The localization turns out to be a consequence of the rapid diffusion of an inhibiting substance occurring in a potentially excitable system. In order to extract the important features of the localized pattern, the method of singular perturbation is employed, with the following results: (1) A stable motionless solitary pattern can exist either for a monostable or bistable system. (2) Under suitable conditions such a pattern undergoes the Hopf bifurcation, leading to a "breathing motion" of the activated droplet.

The analysis is restricted to the one-dimensional case throughout.

### § 1. Introduction

Symmetry-breaking standing structures in cross-inhibiting media,<sup>1)~3)</sup> and travelling excitations in cross-activating media<sup>4)~13)</sup> have been considered to constitute the most basic patterns encountered in non-oscillating reaction-diffusion systems; these giving rise to a variety of spatio-temporal structures, each depending on boundary and initial conditions, dimensionality and so on. A simple question might be posed however: Is the third possibility, a solitary pattern without propagation in an infinite medium, impossible? In the present paper we will show how such a pattern is realized for some classes of systems. There has been some discussion concerning localized patterns in systems of infinite and finite extensions,<sup>14), 15)</sup> yet any soluble example and clear explanation of localization mechanisms appear to be lacking so far.

Qualitatively, the pattern of our concern might be contrasted with the other two as follows. Consider a system composed of an autocatalytic substance  $X$  and its antagonist  $Y$ . Suppose that the local subsystem is such that the equilibrium state of  $X$  is potentially unstable but a small deviation from it is prevented from blowing up because of the change simultaneously induced in the concentration of the inhibitor. Then the corresponding distributed system should be unstable with respect to nonuniform disturbances provided that the diffusion rate of  $Y$  is sufficiently high. This is because the rapid spilling out of  $Y$  from the activated center implies that the depressing force on the autocatalytic increase of  $X$  in this region disappears. Moreover, the resulting excess amount of  $Y$  in the surroundings strongly suppresses the production of  $X$  there, leading to a subsequent instability. Such a process will repeat itself, until finally a stationary pattern spreads over the medium. Gierer and Meinhardt<sup>5)</sup> considered that such a process is crucial to

morphogenesis. If, on the other hand, the onset of the autocatalytic production of  $X$  in itself requires some external stimulus, and if the nullcline  $dX/dt=0$  is represented by a sigmoidal curve, then we have a typical excitable system. In such a case, the triggered autocatalytic production of  $X$  will subsequently act as a triggering stimulus on the surroundings. As a consequence, it is believed that either a pulse or a domain boundary travels through the medium, according as the local subsystem is in a monostable or multistable regime. Implicit in the above statement is the assumption that the second substance  $Y$  plays no role except possibly that of a hysteresis-eliciting parameter. But this is only true if the diffusion rate of  $Y$  is not very high. If, on the contrary,  $Y$  is a rapidly diffusing substance, a situation partly analogous to the morphogenetic case is encountered. Namely, the rapid outflow of  $Y$  from the activated center results in the accumulation of  $Y$  at the leading edge of the propagating activated region. This means that the relationship between the fast foliation<sup>16)</sup> at the wavefront and the sigmoidal manifold adjusts itself until a kind of Maxwell's equal area condition<sup>17), 18)</sup> is realized. Eventually, further propagation is completely blocked. Since the condition for the Rashevsky-Turing type instability<sup>11), 2)</sup> is not fulfilled in this case, a possible consequence will be the formation of a completely localized pattern in an infinite medium.

The first two types of pattern are possible for the Bonhoeffer-van der Pol model supplemented by diffusion under suitable conditions. The same model will therefore be appropriate for studying the third pattern also. For the purpose of supplying the above qualitative argument with an analytically rigorous basis, we shall adopt a piecewise linear version of the BVP model, as was done by McKean,<sup>8)</sup> and Rinzel and Keller<sup>9)</sup> in discussing travelling pulses for the FitzHugh-Nagumo model,<sup>7), 10)</sup> a restricted form of the BVP model.

In § 2, a motionless solitary pattern and its stability will be discussed for nonsingular values of the parameters. In § 3, the method of singular perturbation<sup>18), 19)</sup> is employed, and the equation describing the motion of the wavefront is derived in a closed form as was done by Fife<sup>18)</sup> for different case. On studying the solution, we find that besides the stationary localization, discussed in § 2, a particularly interesting phenomenon occurs, namely, a limit cycle oscillation of the front around its equilibrium position. Further implications of our localized pattern will be discussed in § 4. Throughout the present paper, only a one-dimensional system is considered.

## § 2. The stationary localized solution and its stability

The set of equations considered is

$$\frac{\partial X}{\partial t} = -X - Y + H(X - a) + D_x \frac{\partial^2 X}{\partial x^2} \equiv F_X(X, Y) + D_x \frac{\partial^2 X}{\partial x^2}, \quad (2 \cdot 1a)$$

$$\frac{\partial Y}{\partial t} = bX - cY + D_Y \frac{\partial^2 Y}{\partial x^2} \equiv F_Y(X, Y) + D_Y \frac{\partial^2 Y}{\partial x^2}. \quad (2.1b)$$

Here  $H$  is the Heaviside step function, and the parameters  $a$ ,  $b$ ,  $c$  and diffusion constants  $D_X$ ,  $D_Y$  are assumed to be positive. For the sake of simplicity we further assume

$$0 < a < \frac{1}{2}. \quad (2.2)$$

The nullclines  $F_X=0$  and  $F_Y=0$  are shown in Fig. 1. The piecewise linear FitzHugh-Nagumo model as treated in Refs. 8) and 9) is obtained by putting  $c = D_Y = 0$ , whereas Winfree<sup>10)</sup> carried out a computer simulation for the case  $c=0$ ,  $D_X = D_Y$ , to obtain a two-dimensional spiral pattern. In contrast to these, we are concerned in the present paper with the situation  $D_Y \gg D_X$ .

Besides the fixed point  $(X, Y) = (0, 0)$ , Eq. (2.1) has another spatially uniform, stable fixed point  $(X_0, Y_0)$ ,

$$X_0 = \frac{c}{b+c}, \quad Y_0 = \frac{b}{b+c}, \quad (2.3)$$

provided  $c/(b+c) > a$ . Otherwise, Eq.

(2.1) represents a monostable excitable system. We shall retain, however, the above-defined notation  $X_0$  and  $Y_0$  in the latter case also. Further, we note that the condition

$$X_0 < 2a \quad (2.4)$$

may generally be assumed. This is because the system is symmetric in the sense that the transformations

$$\begin{aligned} X &\rightarrow X_0 - X, \\ Y &\rightarrow Y_0 - Y, \\ a &\rightarrow X_0 - a \end{aligned} \quad (2.5)$$

map the system onto itself except that the original condition, which we assume to be  $X_0 > 2a$ , is replaced by its counter-condition (2.4). Still for reasons to be seen later, we do *not* presently assume (2.4).

Let us now seek a nonuniform steady solution  $(X_s(x), Y_s(x))$  which is loca-

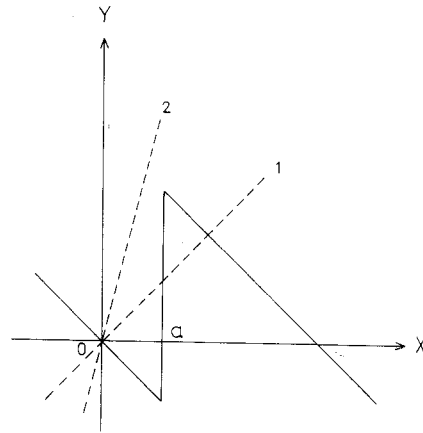


Fig. 1. The nullclines  $F_X=0$  (solid line) and  $F_Y=0$  (broken lines). The lines 1 and 2 correspond to the bistable and monostable cases, respectively.

lized and symmetric around  $x=0$ . Specifically, we require

$$X \cong a \text{ for } |x| \cong \sigma, \quad (2.6)$$

and also the boundary condition

$$X_s(\pm\infty) = Y_s(\pm\infty) = 0. \quad (2.7)$$

Thus the solution under consideration is such that only a small part of the system forms a frozen activated region, while the remaining part is essentially in a homogeneous steady state.

Since the method of finding the solution is analogous to McKean's,<sup>8)</sup> and Rinzel and Keller's,<sup>9)</sup> all the calculational details are omitted below. However the following remarks should be noted. The piecewise linear character of Eq. (2.1) enables us to express the solution in the respective regions, i.e.,  $|x| > \sigma$  and  $|x| < \sigma$ , in terms of linear combinations of exponential functions  $e^{\alpha_i x}$ . Here the  $\alpha_i$  are the zeros of the polynomial

$$P(\alpha) = D_x D_Y \alpha^4 - (c D_x + D_Y) \alpha^2 + b + c. \quad (2.8)$$

Assuming that  $P(\alpha) = 0$  has real roots, as is the case with the parameter values considered later, we have two positive roots  $\alpha_1$  and  $\alpha_2$ , and two negative ones  $-\alpha_1$  and  $-\alpha_2$ . The coefficients of the various exponential functions are determined from the boundary conditions, as are also the matching conditions of  $X_s$  and  $Y_s$  and their first derivatives at  $|x| = \sigma$ . Further, the additional requisite  $X_s(\pm\sigma) = a$  is used for determining  $\sigma$ . In this way we obtain

$$X_s = A_{12} e^{-\alpha_1 x} \cosh(\alpha_1 x) + A_{21} e^{-\alpha_2 x} \cosh(\alpha_2 x) + X_0, \quad |x| < \sigma, \quad (2.9a)$$

$$= -A_{12} \sinh(\alpha_1 \sigma) e^{-\alpha_1 |x|} - A_{21} \sinh(\alpha_2 \sigma) e^{-\alpha_2 |x|}, \quad |x| > \sigma, \quad (2.9b)$$

$$Y_s = \left( D_x \frac{d^2}{dx^2} - 1 \right) X_s + H(\sigma - |x|), \quad (2.9c)$$

where

$$A_{\mu\nu} = \frac{c - D_Y \alpha_\mu^2}{D_x D_Y \alpha_\mu^2 (\alpha_\mu^2 - \alpha_\nu^2)}, \quad \mu, \nu = 1, 2. \quad (2.10)$$

The above solution makes sense only if the condition  $X_s(\pm\sigma) = a$  or, explicitly

$$A_{12} (e^{-2\alpha_1 \sigma} - 1) + A_{21} (e^{-2\alpha_2 \sigma} - 1) = 2a \quad (2.11)$$

has some positive root  $\sigma$ . We shall defer the discussion of the appearance of the stationary pattern for a few paragraphs, and turn now to a consideration of its stability.

The linear stability analysis is also analogous to that of Rinzel and Keller.<sup>9)</sup> Putting into Eq. (2.1) the expressions

$$X = X_s(x) + e^{\lambda t} u(x), \quad (2.12a)$$

$$Y = Y_s(x) + e^{\lambda t} v(x), \quad (2.12b)$$

we obtain a set of variational equations

$$\lambda u = -u - v - \gamma^{-1} \{ \delta(x - \sigma) + \delta(x + \sigma) \} + D_x \frac{d^2 u}{dx^2}, \quad (2.13a)$$

$$\lambda v = bu - cv + D_y \frac{d^2 v}{dx^2}, \quad (2.13b)$$

where

$$\gamma = \frac{dX_s}{dx} \Big|_{x=\sigma}. \quad (2.14)$$

As was the case with  $X_s$  and  $Y_s$ , the eigenfunctions  $u$  and  $v$  are represented in terms of exponential functions  $e^{\beta_i x}$ , however here the  $\beta_i$  are the zeros of

$$\begin{aligned} Q(\beta) &= D_x D_y \beta^4 - \{ D_x(\lambda + c) + D_y(\lambda + 1) \} \beta^2 \\ &\quad + \lambda^2 + (1 + c)\lambda + b + c. \end{aligned} \quad (2.15)$$

The following conditions have now to be imposed: The boundary conditions,  $u(\pm\infty) = v(\pm\infty) = 0$ ; the continuity conditions for  $u$ ,  $v$  and  $dv/dx$  at  $|x| = \sigma$ , and the jump condition

$$\frac{du}{dx} \Big|_{\sigma+0} - \frac{du}{dx} \Big|_{\sigma-0} = (D_x \gamma)^{-1} u(\sigma), \quad (2.16)$$

together with a similar condition at  $x = -\sigma$ . In addition, one may arbitrarily specify the value of  $u$  at, say,  $x = \sigma$ . Most conveniently, one may put

$$u(\sigma) = D_x \gamma. \quad (2.17)$$

In this way  $u$  and  $v$  are easily obtained, the expressions are, however, omitted here. The eigenfunction  $u$  thus obtained is now substituted into Eq. (2.17), which leads to an equation for the eigenvalue:

$$G_+(\lambda) G_-(\lambda) = 0, \quad (2.18)$$

where

$$G_{\pm}(\lambda) = (1 \pm e^{-2\beta_1 \sigma}) f_1 + (1 \pm e^{-2\beta_2 \sigma}) f_2 + \gamma, \quad (2.19a)$$

$$f_{\mu} = \left( -\frac{dQ(\beta_{\mu})}{d\beta_{\mu}} \right)^{-1} (D_y \beta_{\mu}^2 - \lambda - c), \quad \mu = 1, 2, \quad (2.19b)$$

and real parts of  $\beta_1$  and  $\beta_2$  are assumed to be positive. Since  $(X_s(x), Y_s(x))$  is a symmetric pattern, the eigenfunctions must be symmetric or antisymmetric, cor-

responding to  $G_+$  and  $G_-$  respectively. It can readily be checked that the zero value of  $\lambda$  always satisfies Eq. (2.18), in particular,  $G_-(\lambda) = 0$ . This is a natural consequence of the fact that the spatial translation of the original pattern is also a solution of Eq. (2.1).

Figure 2 shows how  $\sigma$ , the root of Eq. (2.11), is obtained graphically. It can be seen that as  $a$  decreases, there is at first no stationary solution, but at  $a = a_c$  a pair of roots  $\sigma_1$  and  $\sigma_2$  appear. Subsequently, at  $a = X_0/2$ , the larger root  $\sigma_2$  disappears. By numerical analysis of Eq. (2.18), we found that the solutions corresponding to the  $\sigma_1$  branch are always unstable. That is, if  $\lambda$  is real, its positive value always corresponds to the  $\sigma_1$  branch as explained in Fig. 3. Thus the situation here is analogous to the travelling wave case discussed by Rinzel and Keller.<sup>9</sup> In particular, their fast pulse and slow pulse solutions may be compared with our localized solutions with large and small pulse width, respectively. This does not necessarily mean, however, that our large width solutions are always stable. In fact, further numerical analysis of Eq. (2.18) shows that such a solution admits, in some cases, a complex eigenvalue with positive real part as is seen from Fig. 3. This implies the interesting possibility that a localized pattern undergoes the Hopf

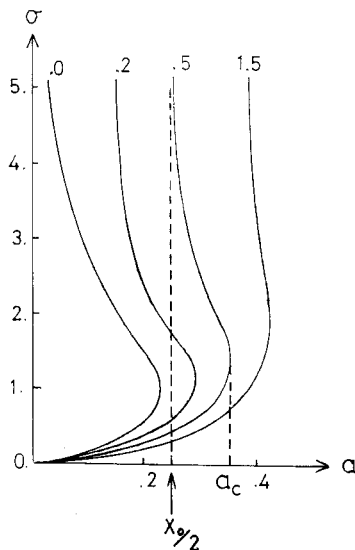


Fig. 2.

Fig. 2. Pulse width  $\sigma$  versus  $a$  for several values of  $c$  (the number attached to each curve), calculated from Eq. (2.11). The parameter values are:  $D_X=1$ ,  $D_T=5$ ,  $b=0.5$ .

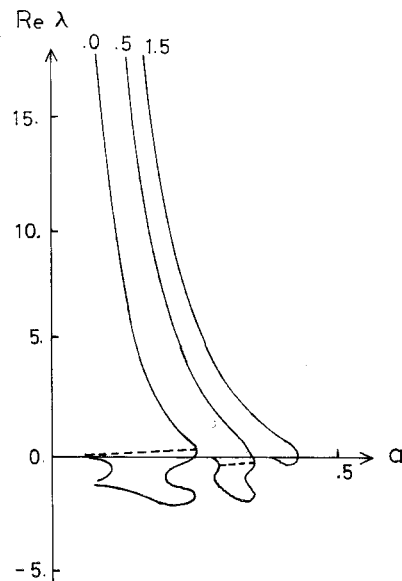


Fig. 3.

Fig. 3. Eigenvalue  $\lambda$  versus  $a$  for several values of  $c$  (the number attached to each curve). The solid lines and broken lines correspond to the real and complex eigenvalues, respectively. The positive part of the solid line corresponds to the  $\sigma_1$ -branch, and the negative part of the same line together with the broken line corresponds to the  $\sigma_2$ -branch.

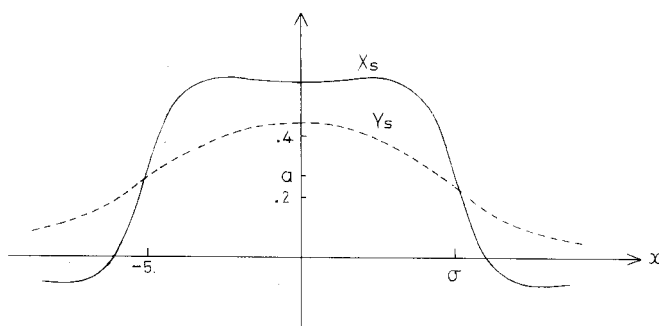


Fig. 4. A localized pattern of the  $\sigma_2$ -branch obtained from Eq. (2.9). The parameter values are:  $D_X=1$ ,  $D_Y=5$ ,  $b=c=0.5$ ,  $a=0.254$ .

bifurcation. This point will further be discussed in § 3.

Figure 4 illustrates the localized pattern of the  $\sigma_2$  branch. Although the corresponding uniform system is in the bistable regime for the assumed parameter values in Fig. 4, essentially the same localized pattern is possible in the monostable regime as well, as we shall see in § 3.

The above stability analysis is still incomplete, especially for complex  $\lambda$ . Nevertheless, it strongly suggests the existence of some stable, motionless solitary pattern under suitable parameter values. In the next section, we take a somewhat different point of view by which one might be led to a clearer understanding of the localization mechanism.

### § 3. Evolution of wavefronts

Let us introduce a small parameter  $\epsilon$  and consider the situation where some of the system parameters are small with some suitable dependence on  $\epsilon$ . Specifically, we are interested in the case

$$D_X = \epsilon \tilde{D}_X, \quad b = \epsilon^\delta \tilde{b}, \quad c = \epsilon^\delta \tilde{c}, \quad -1 < \delta \leq 1. \quad (3.1)$$

Here  $\tilde{D}_X$ ,  $\tilde{b}$  and  $\tilde{c}$  as well as the other parameters are quantities of normal magnitudes. Assuming  $D_X = \epsilon \tilde{D}_X$  implies that the diffusion of the activator is slow, which is equivalent to the fast diffusion of the inhibitor. Further, if  $\delta > 0$ , the assumption (3.1) implies that the sigmoidal manifold may be considered a slow manifold.

By allowing  $\epsilon \rightarrow 0$ , the zeros of  $P(\alpha)$  are reduced to

$$\alpha_1 = 1/\sqrt{\tilde{D}_X} \sim \epsilon^{-1/2}, \quad (3.2a)$$

$$\alpha_2 = \sqrt{(\tilde{b} + \tilde{c})/\tilde{D}_Y} \sim \epsilon^{\delta/2}. \quad (3.2b)$$

Thus we have two characteristic length scales, namely, a very small scale  $\sim \epsilon^{1/2}$ , and a comparatively large scale  $\sim \epsilon^{-\delta/2}$ . If an abrupt spatial variation as expressed

by  $e^{\pm\alpha_1 x}$  is replaced by a discontinuity, the stationary solution (2.9) is greatly simplified. In terms of the scaled coordinate  $\xi$  defined by

$$\xi = \epsilon^{\delta/2} x, \quad (3.3)$$

it is expressed as

$$X_s = Y_0 e^{-\tilde{\alpha}\eta_0} \cosh(\tilde{\alpha}\xi) + X_0, \quad |\xi| < \eta_0, \quad (3.4a)$$

$$= -Y_0 \sinh(\tilde{\alpha}\eta_0) e^{-\tilde{\alpha}|\xi|}, \quad |\xi| > \eta_0, \quad (3.4b)$$

$$Y_s = -X_s + H(\eta_0 - |\xi|). \quad (3.4c)$$

Here  $\tilde{\alpha}$  is defined by

$$\tilde{\alpha} = \epsilon^{-\delta/2} \alpha_2, \quad (3.5)$$

and  $\eta_0$  is the scaled pulse width which is found from Eq. (2.11) to be

$$\eta_0 = \epsilon^{\delta/2} \sigma = \frac{1}{2\tilde{\alpha}} \ln \frac{Y_0}{2a - X_0}. \quad (3.6)$$

Clearly a prerequisite here is that  $2a > X_0$ ; otherwise the transformations (2.5) should be performed on the above solution. In this case an upside-down pattern would be obtained. The above results do not depend on whether the system is in a bistable or monostable regime, as anticipated in the preceding section. A pattern corresponding to the above is illustrated in Fig. 5. It is clear that discontinuities appear only for  $X_s$ . Furthermore the equality

$$-X_s(\xi) - Y_s(\xi) + H(X_s(\xi) - a) = 0 \quad (3.7)$$

holds everywhere except for  $|\xi| = \eta_0$ . In other words, the local state lies on the

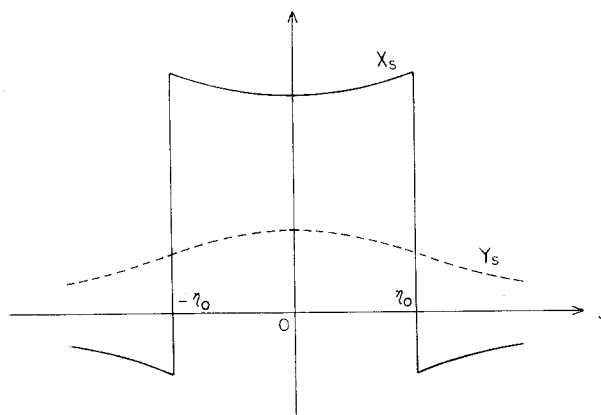


Fig. 5. A localized pattern for the limiting case (3.1). The parameter values are:  $\tilde{D}_x = 1$ ,  $D_T = 1$ ,  $\tilde{b} = 0.5$ ,  $\tilde{c} = 0.5$ ,  $a = 0.3$ .



sigmoidal manifold everywhere except at the front where the motion on the fast foliation occurs. It should be noted that this is true even if  $\delta$  is negative, in other words, for the situation where our sigmoidal manifold is *not* a slow manifold. The fast foliation is represented by

$$Y = \frac{1}{2} - a, \quad (3.8)$$

which fulfils the Maxwell equal-area condition as explained in Fig. 6. In the problem of single front propagation, the equal-area condition is fulfilled only in exceptional cases.<sup>17), 18)</sup> In contrast, for the present case, the system regulates itself until the above condition is satisfied. In order to see how this is possible in an infinite medium, we have now to investigate the dynamical behavior of the front.

As a natural dynamical extension of solution (3.4), let us now seek a symmetric, time-dependent solution of Eq. (2.1) having the following kind of scaled dependence on space and time

$$X = X(\xi, \tau), \quad Y = Y(\xi, \tau), \quad (3.9)$$

where  $\xi$  is defined as before, and

$$\tau = \epsilon^\beta t, \quad \beta > 0 \quad (3.10)$$

with an index  $\beta$ , as yet unspecified. We further assume that the system is in the bistable regime, i.e.,  $X_0 > a$ , and that  $Y(\xi, \tau)$  satisfies  $0 < Y(\xi, \tau) < Y_0$  everywhere. These assumptions remove the complexities arising from the spontaneous splitting of the activated domain as the pattern evolves.

The insertion of the scaled forms (3.9) into Eq. (2.1a) leads to

$$\epsilon^\beta \frac{\partial X}{\partial \tau} = -X - Y - H(X - a) + \epsilon^{1+\delta} \frac{\partial^2 X}{\partial \xi^2}, \quad (3.11)$$

which in the limit  $\epsilon \rightarrow 0$  reduces to

$$X(\xi, \tau) = -Y(\xi, \tau) + H(X(\xi, \tau) - a). \quad (3.12)$$

Of particular interest is again a symmetric solution with a pair of discontinuities. Supposing that the discontinuities occur at  $|\xi| = \eta$ , one may express Eq. (3.12) as

$$X(\xi, \tau) = -Y(\xi, \tau) + H(\eta - |\xi|). \quad (3.13)$$

It is clear that Eq. (3.13) is identical to Eq. (3.4c) if  $\eta$  is replaced by its equi-

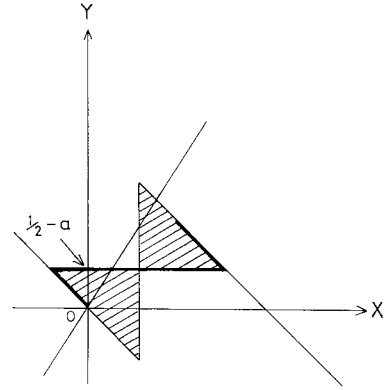


Fig. 6. The local state  $(X_s(\xi), Y_s(\xi))$  traces the bold lines as  $\xi$  is varied. The fast foliation occurs at the discontinuity which corresponds to the horizontal line at  $Y = \frac{1}{2} - a$ . This line divides the sigmoidal nullcline into two shaded regions of equal area.

brium value  $\eta_0$ . In Eq. (3.13), the front position  $\eta$  may still be chosen arbitrarily. However,  $\eta$  turns out to have a certain time-dependence, if we examine the fine structure of the discontinuity. For the assumed scaling form  $X(\xi, \tau)$  to be valid,  $\eta$  should have a scaled time-dependence  $\eta(\tau)$  or, in other words, the scaled instantaneous velocity of the front propagation defined by

$$v = \frac{d\eta(\tau)}{d\tau} \quad (3.14)$$

should be dimensionless in  $\epsilon$ . We shall presently see how this condition determines  $\beta$ .

We have now to investigate the fine structure, the so-called inner solution. For this purpose, it suffices to concentrate on one of the discontinuities, e.g., the one at  $\xi = \eta(\tau)$ . The width of the transition layer around this point is estimated to be

$$\Delta\xi \sim \epsilon^{(1+\delta)/2}, \quad (3.15)$$

as is immediately seen from the balance condition between the diffusion and the other terms in Eq. (2.1a). Thus the appropriate scale of length describing the fine structure is

$$\tilde{\xi} = \epsilon^{-(1+\delta)/2} \xi. \quad (3.16)$$

The coordinate of the discontinuity should also be scaled as

$$\tilde{\eta}(\tau) = \epsilon^{-(1+\delta)/2} \eta(\tau). \quad (3.17)$$

Since  $Y(\epsilon^{(1+\delta)/2} \tilde{\xi}, \tau)$  looks uniform in the  $\tilde{\xi}$  coordinate in the limit  $\epsilon \rightarrow 0$ , it may safely be replaced in Eq. (2.1a) by its value  $Y_\eta$  at the front:

$$Y(\xi, \tau) \rightarrow Y_\eta. \quad (3.18)$$

Introducing a moving coordinate  $z$  as

$$z = \tilde{\xi} - \tilde{\eta}(\tau), \quad (3.19)$$

we now seek the inner solution in the form  $X = X_i(z)$ . Equation (2.1a) now takes the form

$$-\tilde{v} \frac{dX_i(z)}{dz} = -X_i(z) - Y_\eta + H(X_i(z) - a) + \tilde{D}_x \frac{d^2 X_i}{dz^2}, \quad (3.20)$$

where

$$\tilde{v} = \epsilon^\gamma v, \quad (3.21a)$$

$$\gamma = -\frac{1+\delta}{2} + \beta. \quad (3.21b)$$

The inner solution should be such that it may smoothly be continued to the outer solution (3.13), which necessitates the boundary conditions

$$X_i(\infty) = -Y_\eta, \quad (3.22a)$$

$$X_i(-\infty) = 1 - Y_\eta. \quad (3.22b)$$

The solution  $X_i(z)$  is readily found to be

$$X_i(z) = \frac{\alpha_-}{\alpha_+ - \alpha_-} e^{\alpha_- z} + 1 - Y_\eta, \quad z < 0, \quad (3.23a)$$

$$= \frac{\alpha_+}{\alpha_+ - \alpha_-} e^{\alpha_+ z} - Y_\eta, \quad z > 0, \quad (3.23b)$$

where

$$\alpha_\pm = \frac{1}{2\tilde{D}_x} [-\tilde{v} \pm \sqrt{\tilde{v}^2 + 4\tilde{D}_x}], \quad (3.24)$$

and the scaled propagation velocity becomes

$$\tilde{v} = (1 - 2a - 2Y_\eta) \sqrt{\tilde{D}_x / (a + Y_\eta)(1 - a - Y_\eta)}. \quad (3.25)$$

The afore-mentioned requirement for  $v$ , namely, the fact that it is independent of  $\epsilon$ , means  $\gamma = 0$ , or

$$\beta = \frac{1 + \delta}{2}. \quad (3.26)$$

Hence

$$\frac{d\eta}{d\tau} = (1 - 2a - 2Y_\eta) \sqrt{\tilde{D}_x / (a + Y_\eta)(1 - a - Y_\eta)}. \quad (3.27)$$

Equations (3.13) and (3.27) completely establish the interrelation between the outer solutions  $X(\xi, \tau)$  and  $Y(\xi, \tau)$ . Eliminating  $X(\xi, \tau)$  from Eqs. (3.13) and (2.1b), we obtain

$$\epsilon^{(1-a)/2} \frac{\partial Y}{\partial \tau} = -(\tilde{b} + \tilde{c})Y + \tilde{b}H(\eta(\tau) - |\xi|) + D_T \frac{\partial^2 Y}{\partial \xi^2}. \quad (3.28)$$

Solving Eq. (3.28) means that  $Y_\eta$  has been found in terms of  $\eta$ , while Eq. (3.27) describes the evolution of  $\eta$  in terms of  $Y_\eta$ . Thus the elimination of  $Y_\eta$  from these two equations yields the evolution equation of  $\eta$  in a closed form. In solving Eq. (3.28) we have to treat the cases  $-1 < \delta < 1$  and  $\delta = 1$  separately.

*Case 1.*  $-1 < \delta < 1$

Here the left-hand side of Eq. (3.28) may be dropped. Thus the bounded solution may be expressed as

$$Y(\xi, \tau) = -Y_0 e^{-\tilde{\alpha}\eta(\tau)} \cosh(\tilde{\alpha}\xi) + Y_0, \quad |\xi| < \eta(\tau), \quad (3.29a)$$

$$= Y_0 \sinh(\tilde{\alpha}\eta(\tau)) e^{-\tilde{\alpha}|\xi|}, \quad |\xi| > \eta(\tau). \quad (3.29b)$$

By replacing  $\eta(\tau)$  by  $\eta_0$ , the above can be made identical to Eq. (3.4c). The value of  $Y$  at the front is

$$Y_\eta = \frac{Y_0}{2}(1 - e^{-2\tilde{\alpha}\eta(\tau)}), \quad (3.30)$$

which together with Eq. (3.27) describes the approach of  $\eta(\tau)$  to  $\eta_0$ . The equilibrium position  $\eta_0$  may be found by putting  $d\eta/d\tau = 0$  in Eq. (3.27). From this we have  $Y_\eta = \frac{1}{2} - a$ , which, when substituted into Eq. (3.30), correctly yields an expression for  $\eta_0$  identical to that of (3.6). In order to show that  $\eta_0$  represents a stable position of the front, it suffices to show that the inequality

$$d\left(\frac{d\eta}{d\tau}\right)/d\eta < 0 \quad (3.31)$$

holds. However this is evident because we have

$$\frac{dY_\eta}{d\eta} > 0 \quad (3.32)$$

from Eq. (3.30), and

$$d\left(\frac{d\eta}{d\tau}\right)/dY_\eta < 0 \quad (3.33)$$

from (3.27). The inequalities (3.32) and (3.33) clearly show how the localization is possible: The first inequality implies that if, for instance, the activated region expands ( $d\eta > 0$ ), the concentration of the inhibitor observed at the moving front increases. This in turn acts as a decelerating force according to the second inequality. If initially the extension of the activated region is sufficiently small, then it will at first make an expansion ( $d\eta/d\tau > 0$ ) according to the cross-excitatory nature of the system. At the same time, however, the cross-inhibitory nature starts to manifest itself ( $dY_\eta/d\eta > 0$ ). Eventually, the propagation is completely blocked when  $Y_\eta$  attains the value  $\frac{1}{2} - a$ .

*Case 2.  $\delta = 1$*

The term on the left-hand side of Eq. (3.28) is equally as important as the other terms. Still the general solution of that equation is readily found. By taking spatial Fourier transforms,

$$Y_q(\tau) = \int_{-\infty}^{\infty} Y(\xi, \tau) e^{iq\xi} d\xi, \quad (3.34a)$$

$$g_q(\tau) = \tilde{b} \int_{-\infty}^{\infty} H(\eta(\tau) - |\xi|) e^{iq\xi} d\xi = 2\tilde{b}q^{-1} \sin(q\eta(\tau)), \quad (3.34b)$$

Eq. (3.28) is transformed into the set of ordinary differential equations

$$\frac{dY_q}{d\tau} = -r_q Y_q + g_q(\tau), \quad (3.35)$$

where

$$r_q = \tilde{b} + \tilde{c} + D_Y q^2. \quad (3.36)$$

Integrating Eq. (3.35) and taking the inverse Fourier transform of  $Y_q$  lead to

$$Y(\xi, \tau) = \frac{\tilde{b}}{\sqrt{\pi}} \int_0^\tau d\tau' e^{-(\tilde{b} + \tilde{c})\tau'} f(\tau'), \quad (3.37)$$

where

$$f(\tau') = \int_{L_-(\xi)}^{L_+(\xi)} e^{-x^2} dx, \quad (3.38a)$$

$$L_\pm(\xi) = \frac{\xi \pm \eta(\tau - \tau')}{2\sqrt{D_Y \tau'}}. \quad (3.38b)$$

In particular,

$$Y_{\eta(\tau)} = \frac{\tilde{b}}{\sqrt{\pi}} \int_0^\tau d\tau' e^{-(\tilde{b} + \tilde{c})\tau'} \int_{L_-(\eta(\tau))}^{L_+(\eta(\tau))} e^{-x^2} dx. \quad (3.39)$$

As in Case 1, Eqs. (3.27) and (3.39) describe the motion of  $\eta(\tau)$  in a closed form. Its equilibrium value  $\eta_0$  should be identical to (3.6). This may be confirmed as follows. We replace  $\eta(\tau)$  and  $\eta(\tau - \tau')$  by  $\eta_0$  in Eq. (3.39), and let  $\tau \rightarrow \infty$ . Then, by partial integration, we obtain

$$\begin{aligned} Y_{\eta_0} &= \frac{Y_0}{2} \left( 1 - \frac{\eta_0}{\sqrt{\pi D_Y}} \int_0^\infty \exp \left[ - \left\{ (\tilde{b} + \tilde{c}) \tau' + \frac{\eta_0^2}{D_Y \tau'} \right\} \right] \tau'^{-3/2} d\tau' \right) \\ &= \frac{Y_0}{2} \left( 1 - \exp \left[ - 2\sqrt{\frac{\tilde{b} + \tilde{c}}{D_Y}} \eta_0 \right] \right). \end{aligned} \quad (3.40)$$

Noting that the above has a form identical to (3.30), we obtain the same  $\eta_0$  as in Case 1 and hence as in (3.6).

The stability analysis of the above equilibrium position is quite complicated. By putting

$$\eta(\tau) = \eta_0 + \zeta(\tau), \quad (3.41)$$

it is possible to derive a linearized integro-differential equation for  $\zeta$  from Eqs. (3.27) and (3.39), and in principle to determine the eigenvalue  $\lambda$  assuming the asymptotic behavior of  $\zeta(\tau)$  as  $\tau \rightarrow \infty$  to be  $e^{-\lambda t}$ . However, the eigenvalue equation thus obtained turns out to be a couple of quite complicated transcendental equations which makes the further analysis impracticable. Thus we carried out the numerical

time-integration of Eq. (3.27) with the use of (3.39) to study the behavior of  $\eta(\tau)$ . The results may conveniently be described in terms of a parameter  $s$  defined by

$$D_Y = sD_{Y0}, \quad \tilde{b} = s\tilde{b}_0, \quad \tilde{c} = s\tilde{c}_0. \quad (3.42)$$

With  $D_{Y0}$ ,  $\tilde{b}_0$ ,  $\tilde{c}_0$  and the other parameters fixed, we found that there exists a region  $s_2 < s < s_1$  for which a limit cycle oscillation of  $\eta(\tau)$  is possible given appropriate initial conditions. The results are summarized in Fig. 7. At  $s = s_1$ , the Hopf bifurcation occurs. As we decrease  $s$ , the oscillation amplitude becomes larger, and we reach the second critical value  $s_2$  at which the minimum width of the activated domain in the course of the oscillation touches the zero value, so that no persistent oscillation is possible for  $s < s_2$ . This kind of "breathing" of an activated droplet in an infinite medium has not been reported before. Presumably, a qualitative condition for its appearance is a potentially excitable system with slow diffusion rate and production rate of inhibitor. Here the slow production rate of  $Y$  is the only thing which differs from Case 1. Suppose that the activated region has been expanded slightly due to some external effect. Since the production rate

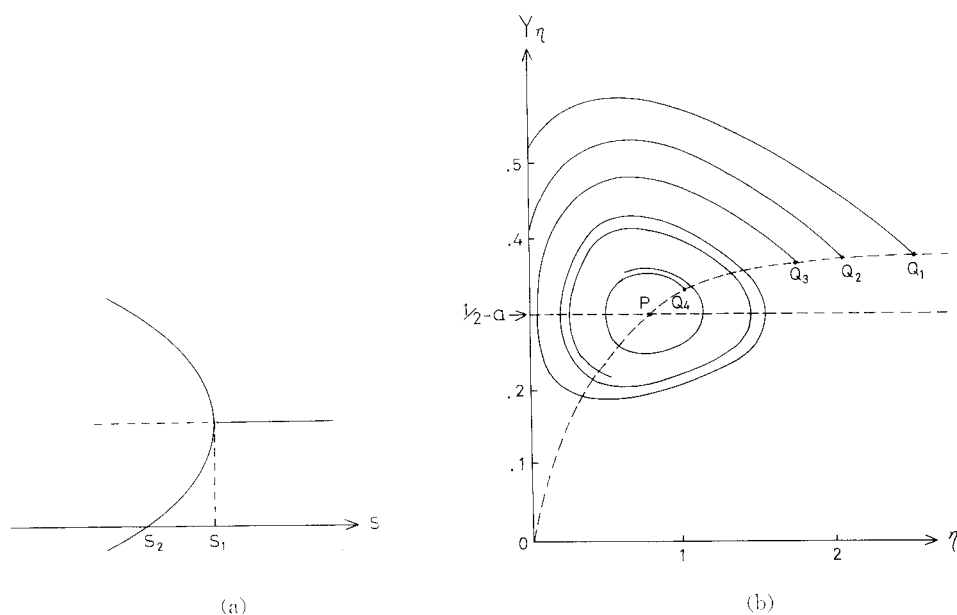


Fig. 7. Limit cycle oscillation of wavefront.

- (a) A schematic bifurcation diagram as a function of  $s$  defined in Eq. (3.42), where the bifurcating branches show the maximum and minimum width of the pulse during oscillation.
- (b) Numerically calculated trajectories on  $\eta$ - $Y_\eta$  plane started with different initial conditions. If the initial state is  $Q_1$  or  $Q_2$ , the pulse collapses and no oscillation is possible; while for  $Q_3$  or  $Q_4$ , a limit cycle oscillation is possible.  $P$  indicates the equilibrium state of the front. The parameter values are:  $\tilde{D}_X = D_Y = 1$ ,  $a = 0.2$ ,  $Y_0 = 0.75$ .

of  $Y$  is slow, the wavefront will at first experience the decrease in  $Y$  as is obvious from Fig. 5. The decrease in  $Y$  accelerates the expansion rate, but the inhibitor  $Y$  will blow up after some time delay. This may be strong enough to push the wavefront backward well beyond its equilibrium position. If such a process repeats itself, we have a limit cycle oscillation.

#### § 4. Discussion

We have shown that the competition between the cross-inhibitory and cross-excitatory tendencies of the system leads to a new class of phenomena. It should be noted that if a system is able to produce one solitary island, it means that the same system is able to exhibit a great variety of patterns, each composed of a number of islands located arbitrarily provided that they are well separated from each other. This is so because the interaction between the islands decreases exponentially with distance, so that the islands will remain practically stationary during the period of most observations. The system has thus acquired a greater flexibility of response to external stimuli. Such a property might find application in the study of organization in living systems. For instance it might add something worth while to the theory of morphogenesis based on reaction and diffusion: the theories so far appear to presuppose that the Rashevsky-Turing symmetry-breaking instability is essentially the sole underlying mechanism of patterning.

On the other hand, excitable media are well at hand in the field of chemistry, e.g., the Belousov-Zhabotinsky reaction system.<sup>20)</sup> A localized pattern as discussed in this paper might be realized in the above system; the only remaining problem seems to be a technical one, namely, the selective control of the diffusivity parameters.

#### Acknowledgements

The authors would like to thank Professor K. Tomita for stimulating discussions, and also to thank Dr. D. Broomhead for his careful reading of the manuscript.

#### References

- 1) N. Rashevsky, *Bull. Math. Biophys.* **2** (1940), 15, 65, 109.
- 2) A. M. Turing, *Phil. Trans. Roy. Soc. London* **B237** (1952), 37.
- 3) G. Nicolis and I. Prigogine, *Self Organization in Nonequilibrium Systems* (Wiley-Interscience, New York, 1977).
- 4) H. Haken, *Synergetics, An Introduction* (Springer, Berlin, Heidelberg and New York, 1978).
- 5) A. Gierer and H. Meinhardt, *Kybernetik* **12** (1972), 30.  
H. Meinhardt and A. Gierer, *J. Cell. Sci.* **15** (1974), 321.
- 6) P. Ortoleva and J. Ross, *J. Chem. Phys.* **63** (1975), 3398.
- 7) H. FitzHugh, in *Biological Engineering*, ed. H. P. Schwan (McGraw-Hill, New York, 1969).
- 8) H. P. McKean, *Adv. in Math.* **4** (1970), 209.

- 9) J. Rinzel and J. B. Keller, *Biophys. J.* **13** (1973), 1313.
- 10) J. Nagumo, S. Arimoto and S. Yoshizawa, *Proc. IRE.* **50** (1962), 2061.
- 11) J. Rinzel, in *Nonlinear Diffusion*, ed. W. E. Fitzgibbon and H. F. Walker (Pitman, London, 1977).
- 12) H. R. Karfunkel and F. F. Seelig, *J. Math. Biol.* **2** (1975), 123.
- 13) A. T. Winfree, in *Theoretical Chemistry* **4** (Academic Press, New York, San Francisco, London, 1978).
- 14) M. Herschkowitz-Kaufman and G. Nicolis, *J. Chem. Phys.* **56** (1972), 1890.
- 15) P. C. Fife, in *Nonlinear Diffusion*, ed. W. E. Fitzgibbon and H. F. Walker (Pitman London, 1977).
- 16) E. C. Zeeman, in *Towards a Theoretical Biology* **4**, ed. C. D. Waddington (University Press, Edinburgh, 1972).
- 17) A. Nitzan, P. Ortoleva and J. Ross, *Faraday Symp. Chem. Soc.* **8** (1974), 241.
- 18) P. C. Fife, *SIAM-AMS Proceedings* **10** (1976), 23.
- 19) R. E. O'Malley, *Introduction to Singular Perturbations* (Academic Press, New York and London, 1974).
- 20) J. Tyson, *The Belousov-Zhabotinsky Reaction, Lecture Notes in Biomathematics* **10**, ed. S. Levin (Springer, Berlin, Heidelberg and New York, 1976).